



Convergence Time towards Periodic Orbits in Discrete Dynamical Systems

Jesús San Martín^{1*}, Mason A. Porter^{2*}

1 Escuela Técnica Superior de Ingeniería y Diseño Industrial (ETSIDI), Universidad Politécnica de Madrid, Madrid, Spain, **2** Oxford Centre for Industrial and Applied Mathematics, Mathematical Institute, University of Oxford, Oxford, United Kingdom

Abstract

We investigate the convergence towards periodic orbits in discrete dynamical systems. We examine the probability that a randomly chosen point converges to a particular neighborhood of a periodic orbit in a fixed number of iterations, and we use linearized equations to examine the evolution near that neighborhood. The underlying idea is that points of stable periodic orbit are associated with intervals. We state and prove a theorem that details what regions of phase space are mapped into these intervals (once they are known) and how many iterations are required to get there. We also construct algorithms that allow our theoretical results to be implemented successfully in practice.

Citation: San Martín J, Porter MA (2014) Convergence Time towards Periodic Orbits in Discrete Dynamical Systems. PLoS ONE 9(4): e92652. doi:10.1371/journal.pone.0092652

Editor: Mark R. Muldoon, Manchester University, United Kingdom

Received: December 26, 2013; **Accepted:** February 3, 2014; **Published:** April 15, 2014

Copyright: © 2014 San Martín, Porter. This is an open-access article distributed under the terms of the Creative Commons Attribution License, which permits unrestricted use, distribution, and reproduction in any medium, provided the original author and source are credited.

Funding: The authors have no support or funding to report.

Competing Interests: The authors have declared that no competing interests exist.

* E-mail: jesus.sanmartin@upm.es (JSM); porterm@maths.ox.ac.uk (MAP)

Introduction

Periodic orbits are the most basic oscillations of nonlinear systems, and they also underlie extraordinarily complicated recurrent dynamics such as chaos [1–5]. Moreover, they occur ubiquitously in applications throughout the sciences and engineering. It is thus important to develop a deep understanding of periodic dynamics.

It is important and common to question how long it takes a point in phase space to reach a stable periodic orbit from an arbitrary initial condition. When studying synchronization and other forms of collective behavior, it is crucial to examine not only the existence of stable periodic orbits but also the time that it takes to converge to such dynamics in both natural and human-designed systems [6–8]. For example, it is desirable to know how long it will take an engineered system that starts from an arbitrary initial condition to achieve the regular motion at which it is designed to work [9,10]. A system can also be perturbed from regular motion by accident, and it is important to estimate how long it will take to return to regular dynamics. Similar questions arise in physics [11,12], biology [6,13,14], and many other areas. It is also important to consider the time to synchronize networks [15–17] and to examine the convergence properties of algorithms for finding periodic orbits [2,18].

To study the problem of convergence time to periodic orbits, let's first consider the Hartman-Grobman Theorem [19,20], which states that the flow of a dynamical system (i.e., a vector field) near a hyperbolic equilibrium point is topologically equivalent to the flow of its linearization near this equilibrium point. If all of the eigenvalues of the Jacobian matrix evaluated at an equilibrium have negative real parts, then this equilibrium point is reached exponentially fast when one is in a small neighborhood of it. To determine convergence time to a hyperbolic equilibrium, we thus need to calculate how long it

takes to reach a neighborhood of the equilibrium from an arbitrary initial condition. After reaching the neighborhood, the temporal evolution is then governed by a linear dynamical system (which can be solved in closed form). An analogous result holds for hyperbolic periodic orbits in vector fields [21]. To turn periodic orbits in vector fields into fixed points in maps, one can use Poincaré return maps, which faithfully capture properties of periodic orbits. A Poincaré map can be interpreted as a discrete dynamical system, so the problem of determining how long it takes to reach a hyperbolic stable periodic orbit from arbitrary initial conditions in a vector field is reduced to the problem of determining how long it takes to reach the neighborhood of a hyperbolic fixed point in a discrete dynamical system.

Our work considers how long it takes to reach a periodic orbit of a differential equation—starting from an arbitrary point in phase space—by using a Poincaré return map of its associated vector field. For simplicity, suppose that a return map (which is built from a Poincaré section) is unimodal. If we approximate the unimodal Poincaré map by using a unimodal function $f(x)$, then we can use $f(x)$ in our algorithm to estimate the convergence time to the periodic orbit. Periodic motion is ubiquitous in models (and in nature), and it is important to explore how long it takes to converge to such behavior.

In this paper, we prove a theorem for the rate of convergence to stable periodic orbits in discrete dynamical systems. Our basic strategy is as follows. We define the neighborhood I_p of a hyperbolic fixed point, and we calculate what fraction ω of the entire phase space I is mapped into I_p after q iterations. Using $\mu(w)$ and $\mu(I)$, respectively, to denote the measures of w and I , a point that is selected uniformly at random from I has a probability of $\mu(w)/\mu(I)$ to reach I_p in q iterations. To illustrate our ideas, we will work with a one-dimensional (1D) discrete dynamical system $x_{n+1} = f(x_n; r)$ that is governed by a unimodal function f and is parametrized by a real number r . We focus on unimodal functions

for two primary reasons: (i) many important results in dynamical systems are based on such functions; and (ii) it is simpler to illustrate the salient ideas using them than with more complicated functions.

To determine the set that is mapped into I_p , we take advantage of the fact that points in periodic orbits are repeated periodically, so their corresponding neighborhoods must also repeat periodically. In theory, an alternative procedure would be to iterate backwards from I_p , but this does not work because one cannot control successive iterations of f^{-1} . The function f is unimodal, so it is not bijective and in general one obtains multiple sets for each backward iteration of a single set. The number of sets grows geometrically, and one cannot in general locate them because an analytical expression for f^{-1} is not usually available.

To explain the main ideas of this paper and for the sake of simplicity, consider a stable periodic orbit O_p of period p that is born in p saddle-node bifurcations of f^p . Every point x_i (with $i \in \{1, \dots, p\}$) of O_p has a sibling point x_i^* that is born in the same saddle-node bifurcation. Because $f^p(x_i) = x_i$ and $f^p(x_i^*) = x_i^*$, it follows that $f^p(I_i) = I_i$, where $I_i = [x_i, x_i^*]$. That is, x_i , x_i^* , and I_i all repeat periodically. Roughly speaking, we will build the interval I_p from the interval I_i .

Consider a plot in which points along the horizontal axis are mapped via f to points along the vertical axis (as is usual for 1D maps). The orbit O_p is periodic with period p , so $x_j \in O_p$ implies that $\{(x_j, f^q(x_j)), q = 0, 1, \dots\}$ yields p periodic points with a horizontal axis location of x_j . We say that these points are located in the "column" x_j . Because $f^q(x_j) = x_i \in O_p$ for some q , we obtain p points located in the same column x_j . These points are given by $\{(x_j, f^q(x_j)) = (x_j, x_i), i = 1, \dots, p\}$. As we have indicated above, each point (x_j, x_i) is associated with an interval I_i . No matter how many iterations we do, the fact that the orbit is periodic guarantees that there are exactly p intervals in the same place (where the points (x_j, x_i) are located). We thereby know the exact number and locations of all intervals.

To complete the picture, we must also take into account that if there exists an interval W_{q_i} such that $f^q(W_{q_i}) = I_i$, then any point of W_{q_i} will reach a point of I_i in at most q iterations. The geometric construction above yields the interval W_{q_i} , as one can see by drawing a pair of parallel line segments that intersect both f^q and the endpoints of the interval I_i . We will approximate f^q by a set of such line segments so that we can easily calculate the intersection points.

The remainder of this paper is organized as follows. First, we give definitions and their motivation. We then prove theorems that indicate how long it takes to reach the interval I_i from an arbitrary initial condition. We then construct algorithms to implement the results of the theorems. Finally, we discuss a numerical example and then conclude.

Definitions

Consider the discrete dynamical system

$$x_{n+1} = f(x_n; r), \quad f : I \rightarrow I, \quad I = [a, b], \quad (1)$$

where $f(x; r)$ is a one-parameter family of unimodal functions with negative Schwarzian derivative and a critical point at $x = C$. Without loss of generality, we suppose that there is a (both local and global) maximum at C . At a critical point of a map f , either $f' = 0$ (as in the logistic map) or f' does not exist (as in the tent map). Some of the results of this paper related with critical points

only require continuous functions, which is a much weaker condition than the requirement of a negative Schwarzian derivative.

Remark 1 Because f has a negative Schwarzian derivative, f^q does as well (because it is a composition of functions with negative Schwarzian derivatives). By using the chain rule, we obtain $f^q = 0$ only at extrema. Therefore, $f^q \neq 0$ between consecutive extrema. The Minimum Principle [22] for a function with negative Schwarzian derivative then guarantees that there is only one point of inflection between two consecutive extrema of f^q . If there were more than one point of inflection, then $f^q = 0$ at least two points. One of them would be a maximum of f^q , and the other one would be a minimum. This contradicts the Minimum Principle. Consequently, the graph of f^q between two consecutive extrema has a sigmoidal shape (i.e., it looks like \int or \backslash), which becomes increasingly steep as q becomes larger. This fact makes it possible to approximate f^q between two consecutive extrema by a line segment near the only point of inflection that is located between two consecutive extrema.

Because the Schwarzian derivative of f is negative, Singer's Theorem [23] ensures that the system (1) has no more than one stable orbit for every fixed value of the parameter r . Additionally, the system (1) exhibits the well-known Feigenbaum cascade [24-26], which we show in the bifurcation diagram in Fig. 1.

For a particular value of the parameter r , the map f^p has p simultaneous saddle-node (SN) bifurcations, which result in an SN p -periodic orbit. As r is varied, the SN orbit bifurcates into a stable orbit $\{S_i\}_{i=1}^p$ and an unstable orbit $\{U_i\}_{i=1}^p$. The points S_i and U_i are, respectively, the node and the saddle generated in an SN bifurcation, so U_i is the nearest unstable point to S_i (see Fig. 2). In other words, the points in the stable orbits (called "node orbits") are node points, whereas the points in the unstable orbit (called "saddle orbits") are saddle points. From Remark 1, we know that the neighborhoods of these points are concave or convex.

The derivative of f^p is 1 at the fixed point where the SN bifurcation takes place. As one varies r , the derivative evaluated at that bifurcation point changes continuously from 1 to -1 . When the derivative is -1 , the stable orbit (i.e., the node orbit) undergoes a period-doubling bifurcation. As a result, the stable orbit becomes unstable (yielding the orbit $\{U_i\}_{i=1}^p$) and two new stable orbits ($\{S_{i_1}\}_{i_1=1}^p$ and $\{S_{i_2}\}_{i_2=1}^p$) appear. The points S_{i_1} and S_{i_2} are nodes, and the point U_i is a saddle. From our geometric approach, the intervals (S_{i_1}, U_i) and (S_{i_2}, U_i) that are generated via the period-doubling bifurcation behave in the same way as the interval (S_i, U_i) that was generated in the SN bifurcation. Therefore, we can drop the indices "1" and "2" and write (S_i, U_i) for the orbits that arise from both the SN bifurcation and the period-doubling bifurcation.

Notation 1 Let U'_i denote the nearest point to S_i that results from the intersection of the line $x_{n+1} = U_i$ with f^p (see Figs. 2, 3, and 4).

Definition 1 Consider the points x_i and x'_i that satisfy $f^p(x_i) = U_i$ and $f^p(x'_i) = U'_i$. If f^p is concave (respectively, convex) in a neighborhood of S_i , we say that $I_{P_i} = (x_i, x'_i)$ [respectively, $I_{P_i} = (x'_i, x_i)$] is the i th capture interval of the stable p -periodic orbit $\{S_i\}_{i=1}^p$ and that $I_P = \bigcup_i I_{P_i}$ is the (aggregate) capture interval of the stable p -periodic orbit $\{S_i\}_{i=1}^p$.

Notation 2 Let $I_{P_i,c}$ denote the subinterval I_{P_i} that contains the critical point C .

From Definition 1, we see for all $x \in I_{P_i}$ that $f^{np}(x) \in I_{P_i}$ and $f^{np}(x) \rightarrow S_i$ as $n \rightarrow \infty$. Iterations of points $x \in I_{P_i}$ are repelled from U_i and U'_i , and they are attracted to S_i . The system (1) is linearizable around the fixed points S_i and U_i . (Observe that $f(U'_i) = U_i$, so we also have control over this point.) Consequently,

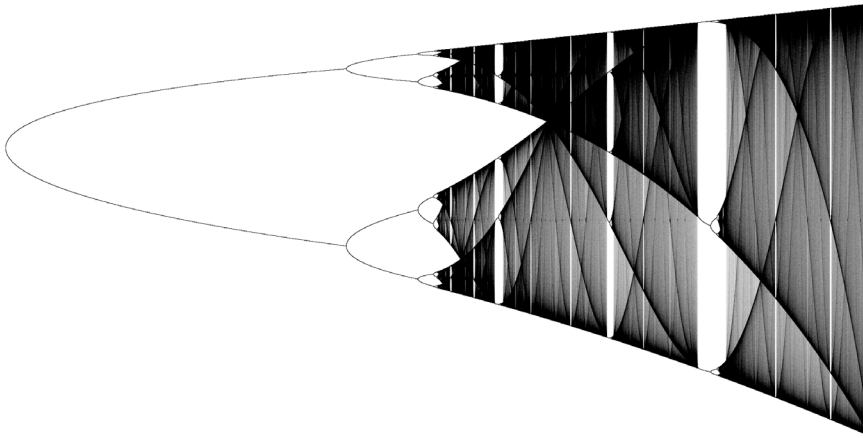


Figure 1. Bifurcation diagram of a unimodal map with a negative Schwarzian derivative. There is a period-doubling cascade on the left, and there are also period-doubling cascades inside several windows (the broad, clear bands) of periodic behavior. Saddle-node orbits arise at the onset of such windows in the chaotic area.
doi:10.1371/journal.pone.0092652.g001

the convergence of iterations of $x \in I_{P_i}$ to S_i is governed by the eigenvalues of the Jacobian matrix Df .

Because we can control the evolution inside I_{P_i} , we can examine how long it takes to reach I_{P_i} , starting from an arbitrary point $x \in I$. As we will see below, to obtain this result, we need to discern which subintervals of I are mapped by f^q into I_{P_i} for arbitrary q . The first step in this goal is to split the interval I in which f^q is defined into subintervals in which f^q is monotonic.

Definition 2 Let $A = \{q_2, q_3, \dots, q_{k-1} \mid q_2 < \dots < q_{k-1}\}$ be the set of points at which f^q has extrema. Let $B = \{q_1 = a, q_k = b\}$, and we

recall that we are considering the interval $I = [a, b]$. We will call $P_{\text{mon-}f} = A \cup B = \{q_1, q_2, q_3, \dots, q_{k-1}, q_k \mid q_1 < q_2 < \dots < q_{k-1} < q_k\}$ the partition of monotonicity of f^q . We will call $I_{q_j} = [q_j, q_{j+1}]$ (where $j = 1, \dots, k-1$) the j th interval of monotonicity of f^q .

By construction, $I = [a, b] = \bigcup_j I_{q_j}$, and f^q is monotonic in I_{q_j} . As

we will explain below, one can calculate intervals of monotonicity I_{q_j} easily by using Lemmas 1 and 2.

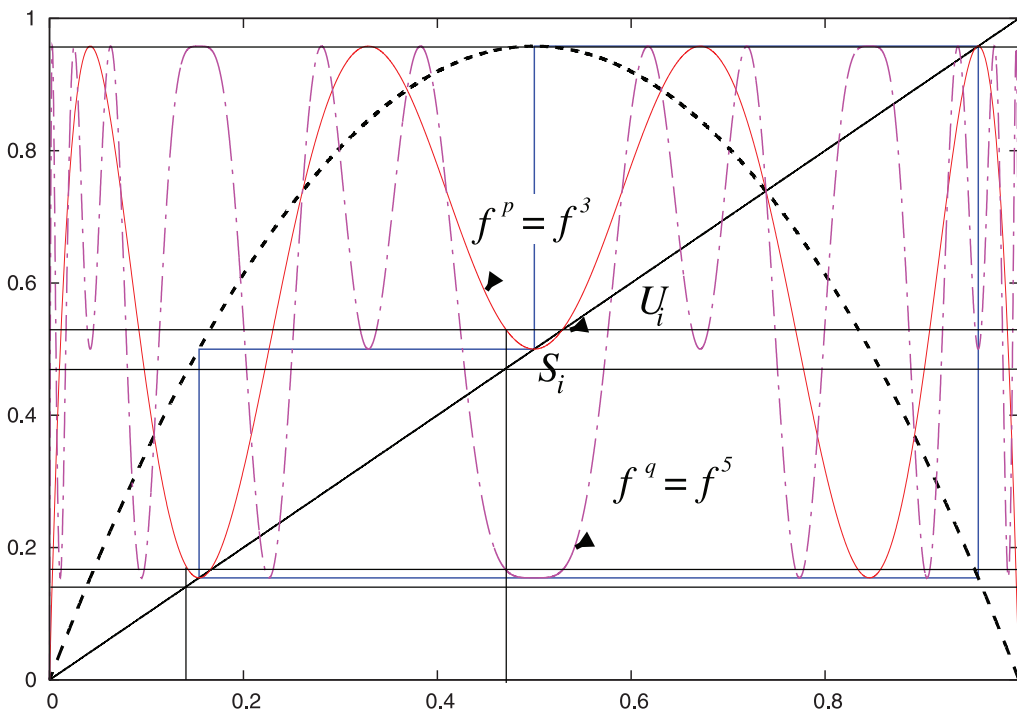


Figure 2. Geometric calculation of the three subintervals W_{q_j} corresponding to a 3-periodic orbit (in blue). See Fig. 3 for a better view of the orbit. These subintervals are determined by the three pairs of black, horizontal, parallel line segments that intersect f^q , U_i , and f^p . (We only indicate one U_i in the figure.) One needs to take into account the intersection points of f^q with all 6 parallel line segments. See Figs. 4 and 5 for more detail. The plot in this figure uses the logistic map. The blue orbit is a period-3 supercycle and $r \approx 3.83187405528331556841$.
doi:10.1371/journal.pone.0092652.g002

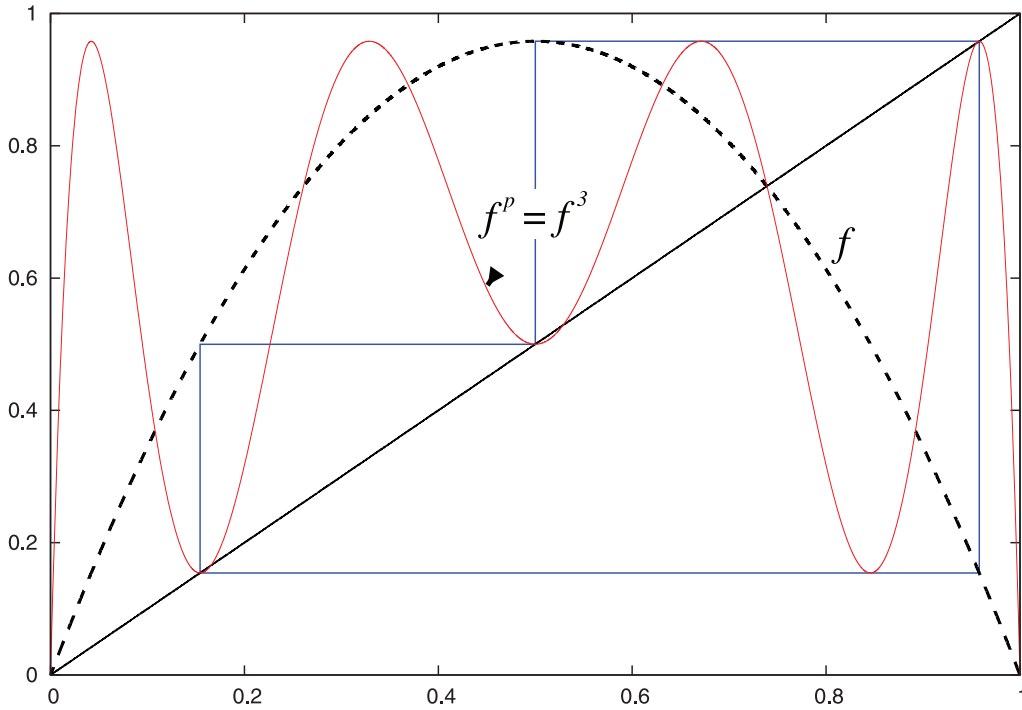


Figure 3. The 3-periodic orbit $f^p = f^3$ from Fig. 2.
doi:10.1371/journal.pone.0092652.g003

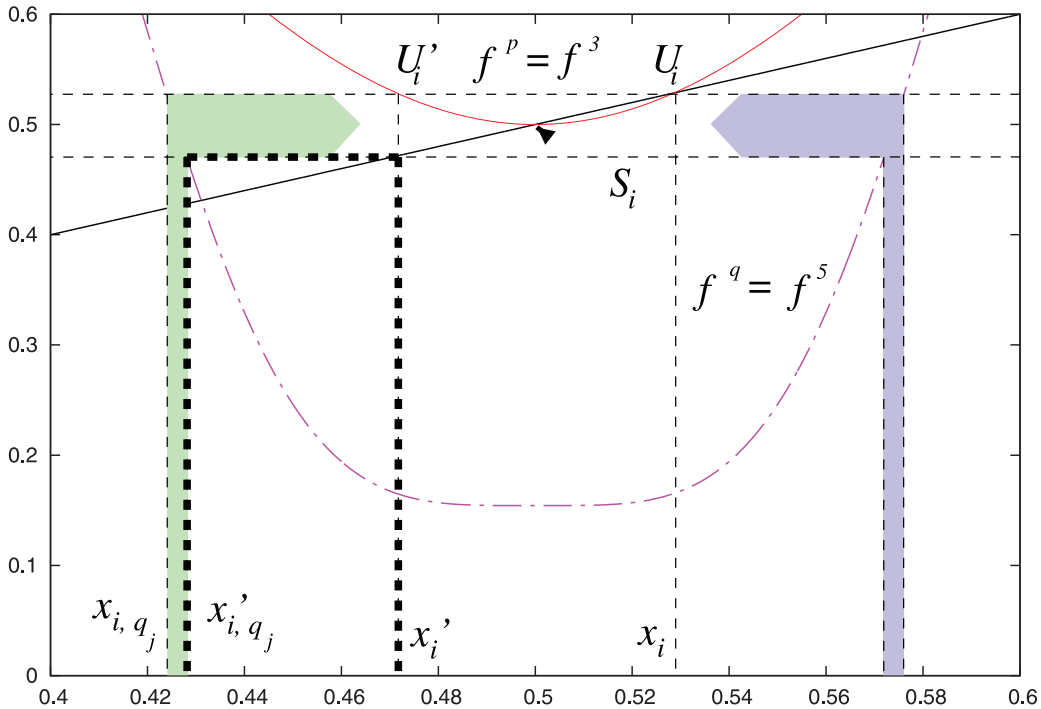


Figure 4. Magnification of Fig. 2. We show the interval W_{q_j} in which f^q does not have any extrema in the region between the horizontal parallel lines. The horizontal line that crosses U_i and intersects with f^p determines U'_i . The vertical lines that intersect U_i and U'_i determine x_i and x'_i , respectively. We obtain locations for the points x_{i,q_j} and x'_{i,q_j} because their images under the map f^q are x_i and x'_i , respectively. We thereby construct the subinterval W_{q_j} . We depict the mapping of the subinterval W_{q_j} using a filled green arrow the mapping of another subinterval using the filled blue arrow.
doi:10.1371/journal.pone.0092652.g004

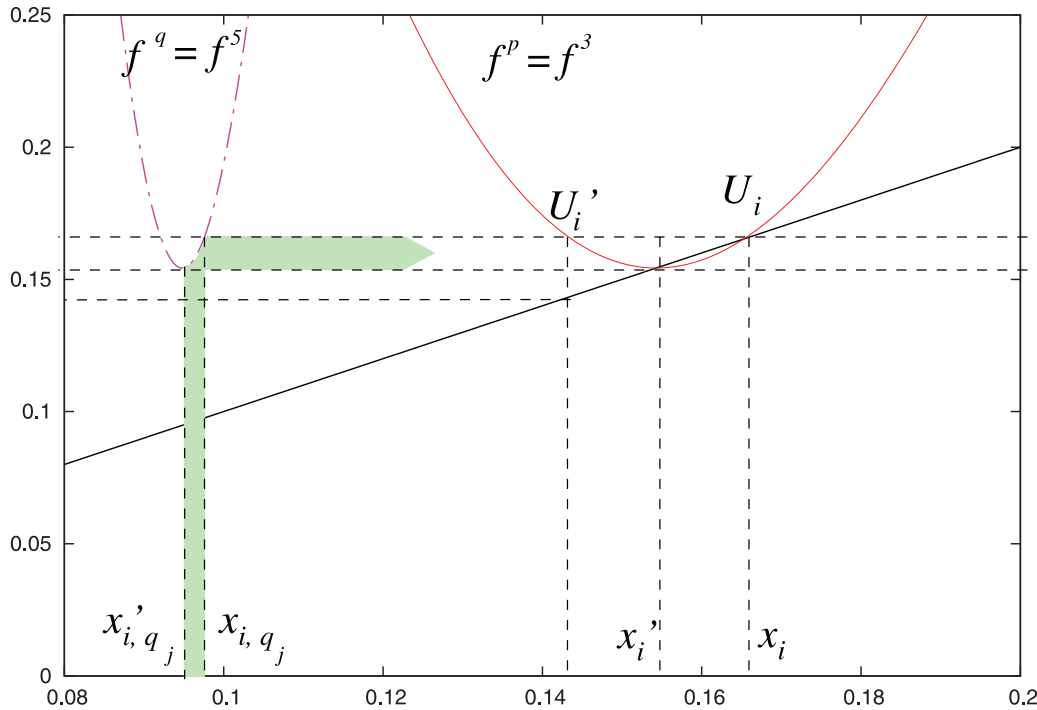


Figure 5. Another magnification of Fig. 2. We show the interval W_{q_j} , in which f^q has an extremum in the region between the horizontal parallel lines. The horizontal line that crosses U_i and intersects f^p determines U_i' . The vertical lines that intersect U_i and U_i' determine the points x_i and x_i' , respectively. We obtain the locations for the points x_{i,q_j} and x'_{i,q_j} because their images under the map f^q are x_i and x'_i , respectively. We thereby construct the subinterval W_{q_j} . We depict the mapping of the subinterval W_{q_j} using a filled green arrow.
doi:10.1371/journal.pone.0092652.g005

Once we know the intervals in which f^q is monotonic, it is easy to obtain subintervals of I that are mapped by f^q into I_{P_i} .

We proceed geometrically (see Figs. 2, 4, and 5):

- draw parallel lines through the points x'_i and x_i (i.e., through the endpoints of I_{P_i});
- obtain the points at which the lines intersect f^q ;
- calculate which points are mapped by f^q into the intersection points of (ii), for which one uses the fact that f^q is monotonic in $I_{q_j} = [q_j, q_j + 1]$;
- determine, using the points obtained in (iii), the interval that is mapped by f^q into I_{P_i} .

Using this geometric perspective, we make the following definitions.

Definition 3 Let

$$A_{ij} = \begin{cases} (x_{i,q_j}, x'_{i,q_j}), & \text{if } x_{i,q_j} < x'_{i,q_j} \\ (x'_{i,q_j}, x_{i,q_j}), & \text{if } x_{i,q_j} > x'_{i,q_j} \end{cases}, \quad (2)$$

where the points $x_{i,q_j}, x'_{i,q_j} \in I_{q_j} = [q_j, q_j + 1]$, and they satisfy $f^q(x_{i,q_j}) = x_i$ and $f^q(x'_{i,q_j}) = x'_i$.

(i) If f^q does not have extrema in A_{ij} (see Figs. 2 and 4), then we let

$$W_{q_{ij}} = A_{ij}. \quad (3)$$

(ii) If f^q has extrema in A_{ij} (see Figs. 2 and 5), then we let

$$W_{q_{ij}} = \begin{cases} (x_{i,q_j}, C], & \text{if } x_{i,q_j} < C \\ [C, x_{i,q_j}), & \text{if } x_{i,q_j} > C \end{cases}. \quad (4)$$

Remark: If we did not take point (ii) into account, then f^q would not be monotonic in W_{q_j} .

By construction, all points $x \in W_{q_j}$ reach I_{P_i} in at most q iterations (see Figs. 2, 4, and 5). That is, $f^l(W_{q_j}) = I_{P_i}$ for $l \leq q$.

Definition 4 We call $W_{R_i} = \bigcup_j W_{q_{ij}}$ the q -capture interval of I_{P_i} , as I_{P_i} is captured after at most q iterations. The interval $W_R = \bigcup_i W_{R_i} = \bigcup_{i,j} W_{q_{ij}}$ is then the q -capture interval of the orbit $\{S_i\}_{i=1}^p$.

Observe that $W_{q_{ij}}$ can be the empty set for some values of j .

Theorems

Once we know W_R , we can calculate the probability that a point picked uniformly at random from phase space is located in W_R . We can then calculate the probability that that point reaches a capture interval of O_p in at most q iterations. We let $\mu(W_R)$ denote the measure of W_R , and we have the following theorem.

Theorem 1 Let $O_p = \{S_i\}_{i=1}^p$ be a stable p -periodic orbit of the system (1). Given an arbitrary point $x \in I$, the probability to reach a capture interval of O_p after at most q iterations is

$$P_q = \frac{\mu(W_R)}{\mu(I)} = \frac{\mu(W_R)}{b-a}. \tag{5}$$

Proof 1 From the definition (4) of W_R , all $x \in W_R$ satisfy $f^l(x) \in I_p$ for $l \leq q$. There always exist values of $l < q$ such that $f^l(x) \in I_p$ because extrema of $f^l(x)$ that satisfy $l < q$ are necessarily also extrema of f^q , and points belonging to the latter set of extrema reach a capture interval of O_p after at most l iterations (see Lemma 1 below). Consequently, one reaches I_p from $x \in W_R$ after at most q iterations (and we note that it need not be exactly q iterations). Thus, the probability to reach I_p from an arbitrary point $x \in I$ after at most q iterations (i.e., the probability that $x \in W_R$) is

$$P_q = \frac{\mu(W_R)}{\mu(I)} = \frac{\mu(W_R)}{b-a}. \tag{6}$$

Corollary 1 With the hypotheses of Theorem 1, the probability to reach a capture interval of O_p in exactly q iterations is

$$P_q - P_{q-1}.$$

This answers the question of how long it takes to reach a capture interval of a p -periodic orbit from an arbitrary point. However, we also need to calculate $\mu(W_R)$. To do this, we need to understand the structure of W_{qj} . As the following lemma indicates, some of these subintervals are located where f^q is monotonic and others contain extrema of f^q .

Lemma 1 If $f : I \rightarrow I$ is an unimodal C^0 function with a critical point at C , then $f^q(x)$ has extrema

- (i) at points for which $f^{q-1}(x) = C$;
- (ii) at the same points at which $f^{q-1}(x)$ has extrema.

Proof 2

(i) For all $x \in I$ such that $f^{q-1}(x) = C$, we know that $f^q(x) = f(f^{q-1}(x)) = f(C)$. Therefore, f^q has an extremum because f has an extremum.

(ii) Write $I = J_L \cup \{C\} \cup J_R$, where $J_L = (a, C)$ and $J_R = (C, b)$, so f is a monotonic function on the intervals J_L and J_R .

(ii.a) If $x \in J_L$ or $x \in J_R$ and the function $f^{q-1}(x)$ has an extremum, then we know that $f^{q-1}(x)$ is a monotonically increasing function on one side of x and a monotonically decreasing function on the other. Consequently, $f^q(x) = f(f^{q-1}(x))$ is the composition of two monotonic functions (f and f^{q-1}), both of which are increasing (or decreasing) on one side of x . On the other side of x , one of them is increasing and the other is decreasing. Therefore, there is an extremum at x .

(ii.b) Otherwise, if $f^{q-1}(x) = C$, then we see straightforwardly that f^q has an extremum.

We have just seen how to determine the locations of extrema of f^q . We also need to know the values that f^q takes at these extrema.

As we will see below, if the system (1) has a stable p -periodic orbit and $q > p$, then the values that f^q takes at its extrema are the same as those that f^p takes at its extrema. This makes it possible to calculate the subintervals W_{qj} that are associated with extrema of f^q by using I_{p_iC} and the derivative of f .

Lemma 2 Let O_p be a stable p -periodic orbit of the system (1). The coordinates of the extrema of f^q (where $q > p$) are $(x_{iC}, f^{q-i}|_p(C))$, where x_{iC} denotes the points $x \in I$ such that $f^i(x) = C$, the index i takes values of $i = 0, 1, \dots, q-1$ (where we note that $f^0 \equiv Id$ is the identity map), and $q-i|_p = (q-i) \bmod p$.

Proof 3 According to Lemma 1, the extrema of f^q are

- (i) $x \in I$ such that $f^{q-1}(x) = C$;
 - (ii) $x \in I$ such that $f^{q-1}(x)$ is an extremum.
- It thus follows that the extrema of f^{q-1} are
- (ia) $x \in I$ such that $f^{q-2}(x) = C$;
 - (iib) $x \in I$ such that $f^{q-2}(x)$ is an extremum.

Repeating the process, we obtain that extrema of f^q are located at x_{iC} , where $i = 0, 1, \dots, q-1$. The value of f^q at x_{iC} is $f^q(x) = f^{q-i}(f^i(x)) = f^{q-i}(C)$.

Because O_p is a stable p -periodic orbit, there exists one point of O_p near C that is repeated periodically after p iterations. Consequently, $\{C, f(C), f^2(C), \dots, f^{p-1}(C)\}$ is a periodic sequence and $f^{q-i}(C) = f^{q-i|_p}(C)$.

Algorithms

As we discussed above, Lemmas 1 and 2 determine intervals of monotonicity (see definition 2), and they also make it possible to construct algorithms for calculating W_{qj} .

For these algorithms, we approximate f^q by line segments in the subintervals in which f^q is monotonic. This approximation is very good unless one is extremely close to an extremum (see Fig. 6), and this is already the case even for relatively small q (as we will demonstrate below). Additionally, recall that W_{qj} is determined by the intersection points of f^q with line segments. Therefore, once we have approximated f^q by a set of line segments, it is straightforward to calculate those intersection points.

Algorithm 1 (Calculating coordinates for extrema of f^q) Suppose that we know the coordinates of the extrema of f^{q-1} . According to Lemma 1, the extrema of f^q are located at the points

- (i) $x \in I$ such that $f^{q-1}(x) = C$ and $f^{q-1}(x)$ is not an extremum;
- (ii) $x \in I$ such that $f^{q-1}(x)$ is an extremum.

We know the extrema in (ii) by hypothesis. To find the extrema in (i), we need to calculate the points $x \in I$ that satisfy $f^{q-1}(x) = C$. Because we know the coordinates of extrema of f^{q-1} , we construct the lines that connect two consecutive extrema (see Fig. 7). Let $x_{n+1} = ax_n + b$ be the equation for such a line. We solve $ax_n + b = C$ to obtain a seed that we can use in any of the many numerous numerical methods for obtaining roots of nonlinear algebraic equations. Observe that f^q is monotonic in the interval in which the line $x_{n+1} = ax_n + b$ is defined. This circumvents any problem that there might otherwise be in obtaining a good seed to ensure convergence of the root solver. Moreover, we have as many seeds as there are points $x \in I$ that satisfy $f^{q-1}(x) = C$. Note that we need to construct both the line that connects $(a, f(a))$ with the first extremum of f^{q-1} and the line that connects $(b, f(b))$ with the last extremum of f^{q-1} .

To calculate the points $x \in I$ for which $f^{q-1}(x)$ is an extremum, we apply this algorithm recursively, and we note that we know by hypothesis that f has an extremum at C . We first build the line segments that connect $(a, f(a))$ with $(C, f(C))$ and $(C, f(C))$ with $(b, f(b))$. These two line segments give seeds from which to determine the points $x \in I$ that satisfy $f(x) = C$. We thereby obtain the coordinates for the extrema of f^2 . We then use the same procedure to obtain the coordinates for extrema of f^3, f^4, \dots, f^q .

We will see below that if the system (1) has a stable p -periodic orbit and $q > p$, then the points $x \in I$ with $f^{q-1}(x) = C$ are given to a very good approximation by the intersection points of two lines. Moreover, as one can see in Fig. 6, the value $q = 6$ is already large enough to approximate f^q very successfully by a set of line segments when f is the logistic map.

Algorithm 2 (Calculation of W_{qj} in the system (1)) Suppose that we know the coordinates of the extrema of f^q (e.g., by computing them using Algorithm 1). We want to obtain W_{qj} from the definition (3), where

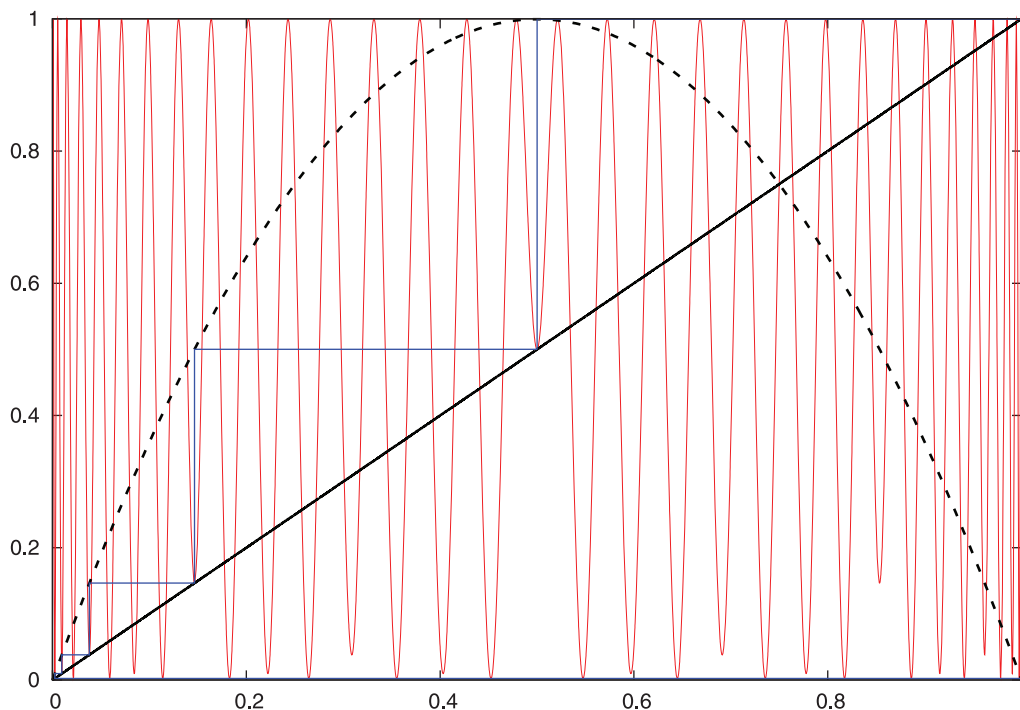


Figure 6. Outside of the intervals W_{q_i} , we approximate the map f^q using line segments. A line segments connects the upper endpoint of the interval W_{q_i} to the lower endpoint of $W_{q_{i+1}}$. The map f^6 is very well approximated using line segments as long as one is not too close to an extremum. We again use the logistic map to illustrate our procedure. The blue curve is a period-6 supercycle and $r \approx 3.99758311825456726610$. See Fig. 7 for a magnification of this figure. doi:10.1371/journal.pone.0092652.g006

$$f^q(x_{i,q_j}) = x_i, \quad f^q(x'_{i,q_j}) = x'_i \tag{7}$$

and the i th capture interval is

$$I_{P_i} = \begin{cases} (x_i, x'_i), & \text{if } x_i < x'_i, \\ (x'_i, x_i), & \text{if } x_i > x'_i. \end{cases} \tag{8}$$

To determine the points x_{i,q_j} and x'_{i,q_j} , we first approximated them by replacing f^q by line segments that connect consecutive extrema of f^q (i.e., by the same procedure that we use in Algorithm 1 to obtain approximations of points). Using the approximations of x_{i,q_j} and x'_{i,q_j} , we construct the interval $I_{app} = (x_{i,q_j}, x'_{i,q_j})$ and then check if there is an extremum of f^q in I_{app} . (This is trivial because we know the coordinates of the extrema of f^q .) We need to consider two cases.

(i) The map f^q has no extrema in I_{app} . This is equivalent to case (i) of Algorithm 1. We use the approximations of x_{i,q_j} and x'_{i,q_j} as seeds in a numerical root-finding method.

(ii) The map f^q has extrema in I_{app} . This is equivalent to case (ii) of Algorithm 1.

If there is an extremum of f^q in I_{app} , then that extremum is necessarily one of the extrema given by Lemma 2: $(x_{iC}, f^{q-i}|_p(C))$. Because $f^i(x_{iC}) = C$ and f is a continuous function, there must exist an interval I_{iC} such that $x_{iC} \in I_{iC}$ and $f^i(I_{iC}) \subset I_{P_i,C}$

Taking into account that x_{iC} is known, we construct the sequence

$$S_{iC} = \{x_{i,0}, x_{i,1}, \dots, x_{i,i} \equiv C\},$$

where $x_{iC} \equiv x_{i,0}$, $x_{i,k} = f^k(x_{iC})$, and $f^0(x_{iC}) = x_{iC}$

Let $L_{i,k}$ be the linear map whose graph is the line of slope $f'(x_{i,k})$ that intersects the point $x_{i,k}$. If the period p of the orbit is sufficiently large, then we can approximate f near $x_{i,k}$ (where $k = 0, 1, \dots, i-1$) by the linear map $L_{i,k}$. Thus, instead of iterating I_{iC} with the map f to obtain $I_{P_i,C}$, we iterate I_{iC} with the linear map $L_{i,k}$ that approximates f . That is,

$$I_{P_i,C} \approx L_{i,i-1} \dots L_{i,0}(I_{iC}).$$

Because each $L_{i,k}$ is a linear map, it is straightforward to compute $L_{i,k}^{-1}$ and hence to compute

$$I_{iC} \approx L_{i,0}^{-1} \dots L_{i,i-1}^{-1}(I_{P_i,C}).$$

At the end of this section, we will discuss the error that is introduced by this approximation.

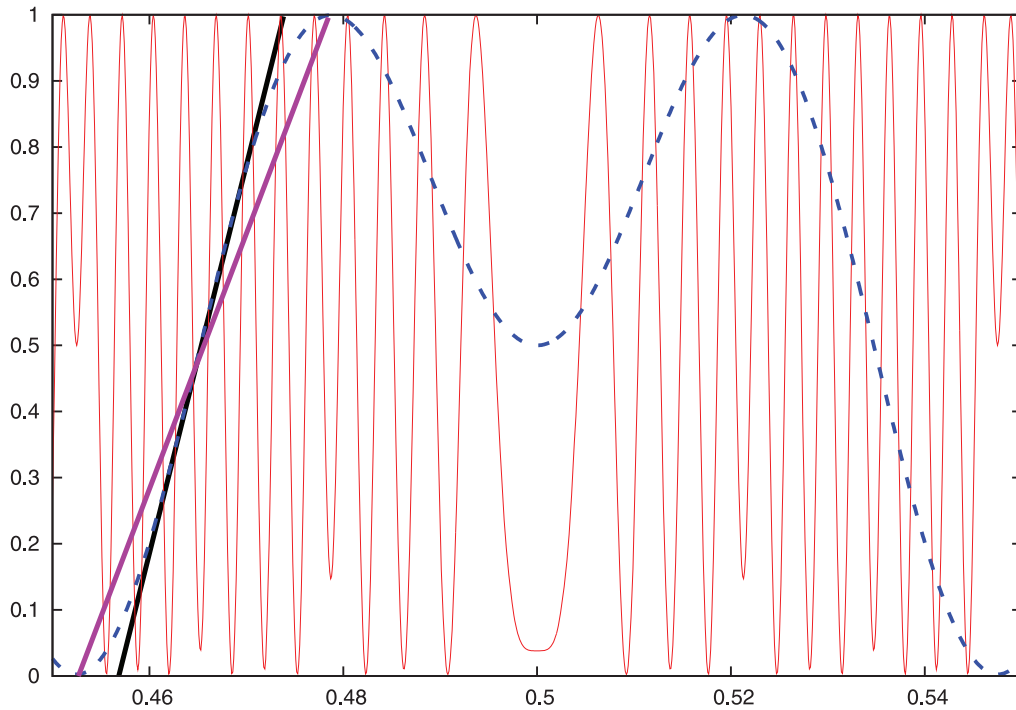


Figure 7. Graphs of f^6 (blue) and f^{10} (red) for the same value of the parameter r (when f is the logistic map) as in Fig. 6. The dark pink line joins two consecutive extrema of f^6 , and the black line is the tangent line that crosses through the inflection point. Both lines are approximations to f^q . As expected, the approximation is better for the larger value of q . doi:10.1371/journal.pone.0092652.g007

The interval I_{iC} that we have just constructed is the interval

$$W_{q_{ij}} = \begin{cases} (x_{i,q_j}, C], & \text{if } x_{i,q_j} < C \\ [C, x_{i,q_j}), & \text{if } x_{i,q_j} > C \end{cases} \quad (9)$$

that we seek.

In Algorithm 1, we constructed line segments that connect two consecutive extrema of f^q . They are located in the intervals $[q_j, q_{j+1})$ and $[q_{j+1}, q_{j+2})$, respectively. We now have intervals $W_{q_{ij}} \subset [q_j, q_{j+1})$ and $W_{q_{i,j+1}} \subset [q_{j+1}, q_{j+2})$ that contain these two consecutive extrema of f^q , so we construct the line segment that connects the upper endpoint of $W_{q_{ij}}$ to the lower endpoint of $W_{q_{i,j+1}}$. (Note that we *do not* connect the two extrema directly via a line segment.) For $q \gg 1$, this line segment approximates f^q outside of the intervals $W_{q_{ij}}$ and $W_{q_{i,j+1}}$. See Fig. 6, which illustrates (for the case when f is the logistic map) that we can approximate f^6 by a set of line segments for $q=6$. We can then use these line segments in Algorithm 1, and we do not need numerical computations to find the intersection points.

As we discussed previously, we can replace f^q by linear expressions to approximate the intersection points when determining W_R in Algorithms 1 and 2. Replacing f^q by a linear approximation simplifies operations and reduces the amount of calculation. To determine the desired intersection points, we have thereby replaced a numerical method for obtaining roots of nonlinear algebraic equations by an analytical calculation that uses a system of two linear equations. We now estimate the error of replacing f^q by lines segments. The line segments that replace the function f^q intersect f^q very close to the unique point of inflection between a pair of consecutive extrema of f^q (see Remark 1 and

Fig. 7). The Taylor polynomial of degree 3 of f^q around the inflection point x_{inf} is

$$f^q(x) \approx f^q(x_{\text{inf}}) + f^{q'}(x_{\text{inf}})(x - x_{\text{inf}}) + \frac{1}{3!} f^{q'''}(x_{\text{inf}})(x - x_{\text{inf}})^3.$$

Consequently, the error of approximating f^q by the line $f^q(x_{\text{inf}}) + f^{q'}(x_{\text{inf}})(x - x_{\text{inf}})$ is

$$\text{Error} = \left| \frac{1}{3!} f^{q'''}(x_{\text{inf}})(x - x_{\text{inf}})^3 \right| \approx \left| \frac{1}{3!} f^{q'''}(x_{\text{inf}}) \left(\frac{b-a}{2^q} \right)^3 \right|, \quad (10)$$

where we have taken into account that there are more than 2^q local extrema of f^q in the interval $[a, b]$. The exponential growth of 2^q enforces a fast decay in the error. Consequently, using line segments to approximate f^q is an effective procedure with only a small error.

Numerical Example

Algorithms 1 and 2 are based on the same procedure: approximate $f^q(x)$ by a line $y(x) = ax + b$ and solve $y(x) = C$ to obtain an approximation of the $f^q(x) = C$ (instead of solving $f^q(x) = C$ directly). In this section, we consider an example application of Algorithm 1.

To obtain the critical points of $f^q + 1$, we need to calculate the points that satisfy $f^q = C$. Suppose that $q=6$ (and again see Fig. 6 for an illustration of the line-segment approximation with $q=6$ for the logistic map). The biggest distance between consecutive

extrema occurs near the critical point C , so we approximate f^6 by a line segment in this region to obtain an upper bound for the error. The extrema are located at $(4.525 \times 10^{-1}, 2.414 \times 10^{-3})$ and $(4.787 \times 10^{-1}, 9.994 \times 10^{-1})$, and they are connected by the line $y \approx 38.053x - 16$, from which we obtain the approximation $x_{\text{app}} \approx 0.453$ for the solution of $f^6(x) = C$. From direct computation, the value of x that satisfies $f^6(x) = C$ is $x \approx 0.465$. The relative error is $E_{\text{rel}} \approx 2.58\%$, and this is the largest error in this example from all of the approximating line segments. As we showed in equation (10), the error decreases exponentially. Hence, when we approximate f^{6+m} using line segments, the relative error will be bounded above by $E_{\text{rel}} \approx 2.58/2^m \%$. One can observe this decrease in error in Fig. 7, in which we plot both f^6 and f^{10} for the logistic map and the same parameter value r . Observe that several extrema of f^{10} lie between consecutive extrema of f^6 , so using the line-segment approximation in f^{10} induces a much smaller error than using it in f^6 .

Conclusions and Discussion

When studying dynamical systems, it is important to consider not only whether one converges to periodic orbits but also how long it takes to do so. We show how to do this explicitly in one-dimensional discrete dynamical systems governed by unimodal functions. We obtain theoretical results on this convergence and develop practical algorithms to exploit them. These algorithms are both fast and simple, as they are linear procedures. One can also apply our results to multimodal one-dimensional maps by separately examining regions of parameter space near each local extremum.

References

1. Moehlis J, Josić K, Shea-Brown ET (2006) Periodic orbit. Scholarpedia 1: 1358.
2. Cvitanović P, Artuso R, Mainieri R, Tanner G, Vattay G, et al. (2012) Chaos: Classical and Quantum. Version 14. Available: <http://chaosbook.org>.
3. Poincaré H (1892–1899) Les méthodes nouvelles de la mécanique céleste. Paris, France.
4. Auerbach D, Cvitanović P, Eckmann JP, Gunarathe G, Procaccia I (1987) Exploring chaotic motions through periodic orbits. *Physical Review Letters* 58: 2387–2389.
5. Artuso R, Aurell E, Cvitanović P (1990) Recycling of strange sets: I. cycle expansions. *Nonlinearity* 3: 325–359.
6. Ermentrout GB, Terman DH (2010) Mathematical Foundations of Neuroscience. New York, NY, USA: Springer-Verlag.
7. Strogatz SH (2000) From Kuramoto to Crawford: exploring the onset of synchronization in populations of coupled oscillators. *Physica D* 143: 1–20.
8. Strogatz SH (1994) Nonlinear Dynamics And Chaos: With Applications To Physics, Biology, Chemistry, And Engineering. New York, NY, USA: Perseus Books Publishing.
9. Lellis PD, di Bernardo M, Garofalo F (2013) Adaptive synchronization and pinning control of networks of circuits and systems in Lurè form. *IEEE Transactions on Circuits and Systems I* in press.
10. Yu W, Lellis PD, di Bernardo M, Kurths J (2012) Distributed adaptive control of synchronization in complex networks. *IEEE Transactions on Automatic Control* 57: 2153–2158.
11. Valtaoja E, Teräsraanta H, Tornikoski M, Sillanpää A, Aller MF, et al. (2000) Radio monitoring of OJ 287 and binary black hole models for periodic outbursts. *The Astrophysical Journal* 531: 744–755.
12. Kreilos T, Eckhardt B (2012) Periodic orbits near onset of chaos in plane Couette ow. *Chaos* 22: 047505.
13. Neufeld Z (2012) Stirring effects in models of oceanic plankton populations. *Chaos* 22: 036102.
14. Sun J, Bollt EM, Porter MA, Dawkins MS (2011) A mathematical model for the dynamics and synchronization of cows. *Physica D* 240: 1497–1509.

Although we have focused on periodic dynamics, the ideas that we have illustrated in this paper can also be helpful for trying to understand the dynamics of chaotic systems. Two important properties of a chaotic attractor are that (i) its skeleton can be constructed (via a "cycle expansion") by considering a set of infinitely many unstable periodic orbits; and (ii) small neighborhoods of the unstable orbits that constitute the skeleton are visited ergodically by dynamics that traverse the attractor [4]. In Refs. [21,22], Schmelcher and Diakonov developed a method to detect unstable periodic orbits of chaotic dynamical systems. They transformed the unstable periodic orbits into stable ones by using a universal set of linear transformations. One could use the results of the present paper after applying such transformations. Moreover, the smallest-period unstable periodic orbits tend to be the most important orbits for an attractor's skeleton [4], so our results should provide a practical tool that can be used to help gain insights on chaotic dynamics.

Once unstable orbits has been transformed into stable ones we can use results of this paper to answer the above question.

Acknowledgments

We thank Erik Bollt, Takashi Nishikawa, Adilson Motter, Daniel Rodríguez, and Marc Timme for helpful comments.

Author Contributions

Analyzed the data: JSM MAP. Wrote the paper: JSM MAP. Proved theorems: JSM MAP. Designed algorithms: JSM MAP. Wrote code and performed numerical simulations: JSM MAP.

15. Qi GX, Huang HB, Shen CK, Wang HJ, Chen L (2008) Predicting the synchronization time in coupled-map networks. *Physical Review E* 77: 056205.
16. Grabow C, Hill SM, Grosskinsky S, Timme M (2010) Do small worlds synchronize fastest? *Europhysics Letters* 90: 48002.
17. Nishikawa T, Motter AE (2010) Network synchronization landscape reveals compensatory structures, quantization, and the positive effect of negative interactions. *Proc Natl Acad Sci USA* 107: 10342–10347.
18. Klebanoff A, Bollt EM (2001) Convergence analysis of Davidchack and Lai Ös algorithm for finding periodic orbits. *Chaos Solitons and Fractals* 12: 1305–1322.
19. Grobman DM (1959) Homeomorphisms of systems of differential equations. *Doklady Acad Nauk SSR* 128: 880–881.
20. Hartman P (1960) On local homeomorphism of Euclidean spaces. *Bol Sc Mat Mexicana* 5: 220–241.
21. Lan Y, Mezic I (2013) Linearization in the large of nonlinear systems and Koopman operator spectrum. *Physica D* 242: 42–53.
22. Brin M, Stuck G (2002) Introduction to Dynamical Systems. Cambridge, UK: Cambridge University Press.
23. Singer D (1978) Stable orbits and bifurcation of maps of the interval. *SIAM Journal of Applied Mathematics* 35: 260–267.
24. Myrberg PJ (1963) Iteration de reellen polynome zweiten grades iii. *Ann Acad Sci Fenn* 336: 1–18.
25. Feigenbaum MJ (1978) Quantitative universality for a class of nonlinear transformations. *Journal of Statistical Physics* 19: 25–52.
26. Feigenbaum MJ (1979) The universal metric properties for nonlinear transformations. *Journal of Statistical Physics* 21: 669–706.
27. Schmelcher P, Diakonov FK (1997) Detecting unstable periodic orbits of chaotic dynamical systems. *Physical Review Letters* 78: 4733–4736.
28. Schmelcher P, Diakonov FK (1998) General approach to the localization of unstable periodic orbits in chaotic dynamical systems. *Physical Review E* 57: 2739–2746.